Measurements and modeling study of intermediates in ethanol and dimethy ether low-pressure premixed flames using synchrotron photoionization

ARTICLE *in* COMBUSTION AND FLAME · SEPTEMBER 2011

Impact Factor: 3.08 · DOI: 10.1016/j.combustflame.2011.01.004

5 AUTHORS, INCLUDING:

Chunde Yao
Tianjin University
138 PUBLICATIONS **772** CITATIONS
SEE PROFILE

Kuiwen Zhang
National University of Ireland, Galway
19 PUBLICATIONS **370** CITATIONS
SEE PROFILE

Huijun Guo
University of Science and Technology of Ch…
17 PUBLICATIONS **259** CITATIONS
SEE PROFILE

Combustion and Flame 158 (2011) 1673–1681

Contents lists available at ScienceDirect

Combustion and Flame

journal homepage: www.elsevier.com/locate/combustflame

Measurements and modeling study of intermediates in ethanol and dimethy ether low-pressure premixed flames using synchrotron photoionization

Hanjun Xu [a], Chunde Yao [a,*], Tao Yuan [b], Kuiwen Zhang [b], Huijun Guo [b]

[a] State Key Laboratory of Engines, Tianjin University, Tianjin 300072, China
[b] National Synchrotron Radiation Laboratory, University of Science and Technology of China, Hefei 230029, China

ARTICLE INFO

Article history:
Received 22 October 2010
Received in revised form 4 January 2011
Accepted 7 January 2011
Available online 1 February 2011

Keywords:
Premixed laminar flame
Synchrotron radiation photoionization
Modeling
Dimethyl ether
Ethanol

ABSTRACT

A molecular-beam flame-sampling photoionization mass spectrometer, employing synchrotron radiation, was applied to detect new intermediates and to measure mole fractions in the low-pressure laminar premixed stoichiometric ratio dimethyl ether (DME)/O_2/Ar and ethanol/O_2/Ar flames respectively. With the help of the means mentioned above, flame species of the two fuels, including isomeric intermediates, were unambiguously identified and the temperature profiles and mole fraction profiles of intermediates were also compared and analyzed. Additionally, five detailed oxidation mechanisms were applied to the modeling study to verify current mechanism for the two fuels. Based on the comparative experimental and modeling study of the two flames at low pressure, the oxidation mechanism for DME and ethanol was revised and a new one was suggested in the present work. The results calculated by the revised mechanism showed that the modeling prediction agreed with those experimental results measured in DME and ethanol flames as well as with the ones in five flames from the experiments done by the other people. In the measurement all species with mole fraction higher than 10^{-4} were considered, including those which have not been included in the present five mechanisms. Meanwhile, the mole fractions of the species which had not been considered by current mechanism such as ethenol, acetone and ethyl methyl ether (EME) were also included in the modeling study. Besides, the reaction paths and species conversion ratio analysis were also conducted to show the difference before and after the mechanism revised.

1. Introduction

Dimethyl ether (DME) and ethanol are isomers, and are both potential clean fuels to substitute for petroleum fuels which have been subjected in much research works. Both of them have low emissions, particularly the significantly low level of soot [1–3]. However their properties show great differences due to their different chemical structures (Table 1). Gaseous DME as a fuel with high cetane number can be applied to compression ignition engines while liquid ethanol as a fuel with high octane number can be applied to spark ignition engines. Because of their different molecule structures, these two fuels with opposite ignition properties not only show their different oxidation behaviors at low temperature, but also their different combust behaviors at high temperature. Therefore, it is worth to investigate into the reaction characteristics of two isomers which have the same atoms composition structure and the similar enthalpy of formation comparatively. The laminar flame is a common way to probe in the combustion intermediates and to test the high temperature oxidation mechanism. By using this method DME and ethanol have been studied by many other researchers, either individual, comparison between each other or mixing with other fuels [4–10]. Several types of instrument include laser and molecular beam mass spectrometry, electron impact ionization mass spectrometry have been used. Recently vacuum ultraviolet (VUV) synchrotron photoionization combining with mass spectrometry which has a high resolution was used to detect the intermediates and calculate their mole fractions in the flames. For example, Cool et al. [8] studied the DME premixed flame and developed a method to calculate the mole fraction of each species; Wang et al. [9] conducted the further modeling study on several equivalence ratio DME samples using the recent DME oxidation kinetic model [11]; In another study Wang et al. [10] investigated the flames of blends of propylene/DME and blends of propylene/ethanol on flame characteristics and the formation of benzene as well as its precursors. Although richer ($\Phi = 2.0$) pure DME and pure ethanol flames were compared experimentally in their study, no modeling study was conducted further. Apart from that, there is not any other comparative modeling study having been seen yet. As DME and ethanol are getting more and more widely used now even in the future and the accurate simulations for both of them still have room to be improved at present time, the modeling study needs to proceed deeply to make

* Corresponding author. Fax: +86 22 2738 3362.
E-mail address: arcdyao@tju.edu.cn (C. Yao).

0010-2180/$ - see front matter © 2011 The Combustion Institute. Published by Elsevier Inc. All rights reserved.
doi:10.1016/j.combustflame.2011.01.004

Table 1
The properties of DME and ethanol [3] (1 atm condition for the measurement of boiling point; 1 atm, 298 K condition for the measurement of low heating value).

Fuel	Boiling point (°C)	Low heating value (MJ kg^{-1})	Cetane number	Octane number
DME	−24.9	27.60	>55	–
Ethanol	78	26.75	<8	108

them more completed. The aim of this study is to investigate into the intermediates in the flames by using synchrotron radiation equipment [12–14], and to develop a kinetic model for the two fuels based on recent kinetic mechanisms and the data from measurement.

2. Experiment and simulation methods

The experiments were carried out at the combustion and flame endstation of the National Synchrotron Radiation Laboratory (NSRL) in Hefei, China. The instruments performing with the experiment have been reported elsewhere [15–18]. Briefly, the instrument consists of a low-pressure flat-flame burner combining with molecular-beam sampling and a reflection linear time of flight mass spectrometer (RTOF-MS) employing VUV synchrotron radiation photoionization. The RTOF-MS was operated at a mass resolving power of $m/\Delta m \approx 1400$. Movement of the burner towards or away from the quartz sampling cone allows the TOF mass spectrum to be taken at any desired position in the flame with a spatial resolution of about 0.5 mm.

Experimental conditions are listed in Table 2. Both of DME and ethanol flames at a pressure of 30 Torr (4.0 kPa) with stoichiometric ratio were chosen for study. The PIE (Photoionization Efficiency) spectra which were used to identify the intermediates with the same mass–charge ratio were obtained at a selected burner position of 1.5 mm. The scan photon energy range is from 8.1 eV to 10.5 eV. Error of measured IE (Ionization Energies) is 0.05 eV for the species with strong signals and 0.1 eV for those with weak signals. Mole fractions of flame species were derived according to the method described by Cool et al. [19]. Photoionization cross sections and mass discrimination factors of most intermediates are shown in Table 3. For stable species the uncertainty should be ±25%, and ±40% for the intermediates with estimated cross section value and radicals. The flame temperature was measured by using a Pt–6%/Rh/Pt–30%Rh thermocouple with a diameter of 0.1 mm. The thermocouple was coated with Y_2O_3–BeO anti-catalytic ceramic to inhibit the catalytic effects [24,25]. The temperature was corrected for the radiation heat loss [26] and cooling effects of sampling nozzle [27]. The uncertainty of the maximum flame temperature was estimated to be ±100 K, which will lead to prediction errors of the present model within 3% for major flame species and 10% for intermediate. Considering the fact that probe samples gases slightly at upstream of the sampling cone orifice [28,29] and the uncertainty (including the spatial resolution, the uncertainty of the position of height zero, absolute position difference between cold or hot conditions and so on) of the distance from the orifice to the burner surface up to 1.0 mm [30]. the "distance from burner" for recorded mole fractions is taken to be 0.5 mm for the sampling cone less than the actual separation between the burner and the tip of the sampling cone in this study. This shift obtains a good agreement of the maximum mole fractions positions between experiment and modeling for most species.

Table 2
Experimental conditions of DME and ethanol premixed laminar flames in the low pressure.

	Flow rates (slm)			Mass flux (g cm^{-2} s^{-1})	Velocity (473 K) cm s^{-1}
	Fuel	O_2	Ar		
DME	0.425	1.275	0.800	0.002429	75.4
Ethanol	0.425	1.275	0.800	0.002429	75.4

Table 3
Photoionizaiton cross sections $\sigma(E)$ and mass discrimination factors $D(M)$.

Species	$\sigma(E)$ (Mb)	$D(M)$	Ref.
CH_3	6(11 eV)/5.6(10)	0.57	[20]
CH_4	4.38(13.18)	0.58	[21]
C_2H_2	38.98(13.18)/23.55(11.8)	0.65	[22]
C_2H_4	8.3(11.8)/7.79(11)	0.70	[22]
C_2H_6	4.38(11.8)	0.76	[21]
CH_2O	10.92(11.8)/9.2(11)	0.76	[23]
CH_3OH	3.63(11)	0.80	[22]
C_2H_2O	6.7(10, Estimated)	1.00	See text
CH_3CHO	7.96(11)	1.04	[12]
C_2H_3OH	6.4(10)	1.04	[12]
CH_3COCH_3	9.18(10)	1.25	[22]
$C_2H_5OCH_3$	10(11, Estimated)	1.27	See text

The PREMIX code was introduced to simulate the flame [31], and temperature profiles were regarded as the input data. The thermal diffusion (Soret effect) was considered, and the transport properties were calculated using the multicomponent formulations. An in-house code for post process was used to analyze the reaction paths and to calculate the conversion distribution rates. To verify the modeling prediction of present mechanisms, a comprehensive modeling study is indispensable, so that five kinetic mechanisms were adopted in this study. They are respectively a DME mechanism developed by Kaiser et al. [32]; an ethanol mechanism developed by Marinov [33]; a DME oxidation mechanism developed recently by Zhao et al. [11], including a series of ethanol dehydrogenation and decomposition reactions developed by Li et al. [34]; the ethanol oxidation mechanism developed by Saxena and Williams [35]; as well as the GRI 3.0 mechanism [36], which was then developed by combining with the DME sub-mechanism in Zhao's mechanism and ethanol sub-mechanism in Li's mechanism. All of these mechanisms have been validated in the experiments of premixed flame, shock tube, flow reactor and jet stirred reactor except the Saxena's mechanism. The validation of this mechanism in flow reactor and jet stirred reactor has not been done yet but counterflow flame experiment as supplement. For DME there has been some new laminar flame study using synchrotron radiation photoionization technique as mentioned above. However, rare ethanol flame study by using this new technique can be seen, let alone the comparative study. The DME sub-mechanism in Zhao's mechanism was also adopted in the Saxena's mechanism so that the DME flame can also be simulated by Saxena's mechanism. As the rate coefficients of $C_2H_5OH + M{=}CH_3 + CH_2OH + M$ and $C_2H_5OH + M{=}C_2H_4 + H_2O + M$ in Zhao's mechanism cannot be applied to low pressure, they were replaced by that in Saxena's mechanism which suits the pressure low to 10^{-2} bar (about 7.5 torr). By analyzing the modeling study results, some of the reactions or the rate parameters in Zhao's mechanism were suggested to be replaced by that in other mechanisms to fit the experiment results better. Detailed revision and the additional thermodynamic data as well as the transport data of new species are given as the Supplementary material 1.

3. Results and discussion

3.1. Species identification

The PIE spectra of mass 44 and 58 in the DME and ethanol flames are shown in Fig. 1. Enols are found to be common

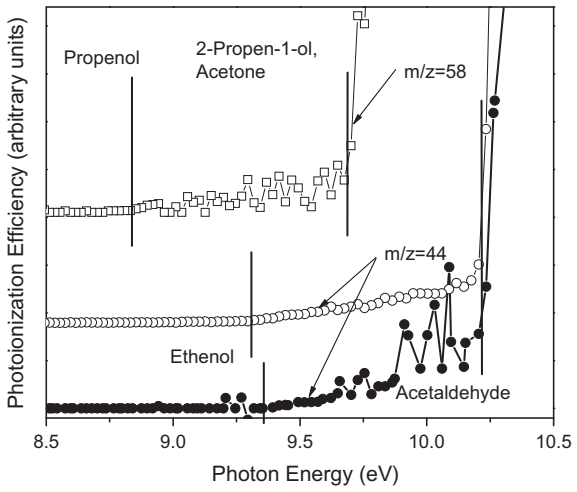

Fig. 1. PIE spectra for enols identification in DME and ethanol flames. The solid symbol stands for DME, the hollow symbol for ethanol.

intermediates of most flame intermediates pool recently [37], and also existed in these two flames. In the DME flame, the lower threshold is 9.35 eV (9.31 eV in the ethanol flame), it was confirmed to belong to the trace amount of ethenol by comparing with the reference data (9.33 ± 0.05 eV) from the NIST Chemistry WebBook [38]. The turning point near 10.22 eV (also 10.22 eV in the ethanol flame, ref. 10.22 ± 0.01 eV) corresponds to the photoionization threshold of acetaldehyde. In the ethanol flame 1-propenol with a threshold of 8.74 eV (ref. 8.70 ± 0.03 eV) and acetone or 2-propen-1-ol with a threshold of 9.70 eV (ref. 9.703 ± 0.006 eV for acetone and 9.67 ± 0.03 eV for 2-propen-1-ol) were detected. With the same method, other intermediates can be confirmed. Some radicals such as ethyl and formyl radical who have the same molecular weight and nearly the same photoionization thresholds are difficult to be distinguished, so the calculation of their mole fractions will not be considered in this work.

3.2. Temperature and mole fraction profiles of major products

Measured temperature profiles and the experimental and modeling mole fraction profiles of major products are shown in Fig. 2. Overall, the temperature profiles are almost the same as expected since both flames were conducted under the same experimental conditions and their fuel thermal values are approximate. The experimental and modeling mole fraction profiles of major species fit very well, so there is no need to modify current mechanisms. In both flames, fuels are almost burnt out at 3 mm and the oxygen concentration decreases sharply to 0.1–0.07 (mole fraction), then reaches approximately steady state at the position of 5 mm where the temperatures reach their peaks. The same species profiles in both flames are very consistent at the end position where their final flame temperatures and the experiment conditions are almost both the same.

3.3. Mole fraction profiles of intermediates

Mole fraction profiles of intermediates were calculated and were classified by their carbon numbers. Those species with their mole fraction less than 10^{-4} were neglected for their less importance.

3.3.1. C_1 intermediates

The mole fractions of some C_1 species, methyl radical (CH_3), methane (CH_4), formaldehyde (CH_2O) and methanol (CH_3OH) are shown in Fig. 3. The results show that the peak concentration of methyl in the DME flame is two times as larger as it in the ethanol flame. The accurate prediction of methyl concentration is significant in the soot formation when DME is blended with some hydrocarbon fuel, although DME itself has little soot emission and it also has higher efficiency at soot reduction than ethanol under low temperature [3], according to the synergistic effect opinion of Yoon [39] and McEnally and Pfefferle [40], DME may cause a higher soot emission than ethanol does when it mixed with some C2 hydrocarbon such as ethylene because of its high methyl concentration. The concentrations of methyl radical and methane in the DME flame have a well prediction, however, all of the previous models have a lower methane concentration prediction and a slightly higher prediction for methyl in the ethanol flame, probable reason is that dehydrogenation reaction of ethanol or acetaldehyde by methyl radical (e.g. $C_2H_5OH + CH_3 = C_2H_4OH + CH_4$, $CH_3HCO + CH_3 = CH_2HCO + CH_4$) was underestimated. The previous flow reactor experiment also shows the similar behaviors, and the rates were increased by a factor of 2 to bring the concentration of methane within the uncertainty region in that study [41]. So the A-factors of dehydrogenation reactions of ethanol by methyl ($C_2H_5OH + CH_3 = C_2H_4OH + CH_4$, $C_2H_5OH + CH_3 = CH_3CHOH + CH_4$, and $C_2H_5OH + CH_3 = CH_3CH_2O + CH_4$) were amplified by a factor of 5 in the revision to obtain a good prediction, but this revise needs more theoretical and experimental test. The peak concentration of formaldehyde in the DME flame is higher than that in the ethanol flame, and the predictions of all the models are similar to each other, also the revised version. Figure 3d shows the mole fraction of methanol. In the revised mechanism the reaction coefficient of "$CH_3 + OH + [M] = CH_3OH + [M]$" was replaced by that in Kaiser's mechanism and has a better prediction. But methanol was all underestimated greatly in the DME flame. Wang et al. [9] also got the similar result, and it was attributed to missing reactions or experimental measurement uncertainties. Here the measurement uncertainties seem to be not possible since it has a well prediction in the ethanol flame. Generally methanol is the by-product in those flame, and is formatted by the reaction path of $CH_3 \rightarrow CH_3O \rightarrow CH_3OH$. According to the experiment results, a wanting describe of a shortcut from DME to methanol is probable. Further revision cannot be conducted since the lack of elementary reactions research.

3.3.2. C_2 intermediates

Figure 4 shows the mole fractions of some C_2 intermediates including species in the predominating path such as ethane (C_2H_6), ethylene (C_2H_4), acetylene (C_2H_2), acetaldehyde (CH_3CHO) and others in the branch path such as ketene (C_2H_2O) and ethenol (C_2H_3OH). As ethane and formaldehyde have the very similar molecular weights, the ethane signal might be covered by the formaldehyde signal in the mass spectrum, causing that they cannot be separated directly. However, because the photoionization thresholds of ethane and formaldehyde are 11.52 eV and 10.88 eV respectively [38], based on the method developed by Cool et al. [19], the following method was developed to calculate their mole fractions:

1. Calculate the mole fraction of CH_2O at the photoionization energy of 11.0 eV.

$$X_{CH_2O} = \frac{S(11)_{CH_2O} X_{C_2H_4} \sigma(11)_{C_2H_4} D_{C_2H_4}}{S(11)_{C_2H_4} \sigma(11)_{CH_2O} D_{CH_2O}}$$

Here $S(11)_{CH_2O}$ and $S(11)_{C_2H_4}$ are the ion signals, $X_{C_2H_4}$ is the mole fraction of C_2H_4, $\sigma(11)_{C_2H_4}$ and $\sigma(11)_{CH_2O}$ are the photoionization cross section, $D_{C_2H_4}$ and D_{CH_2O} are the mass discrimination factors.

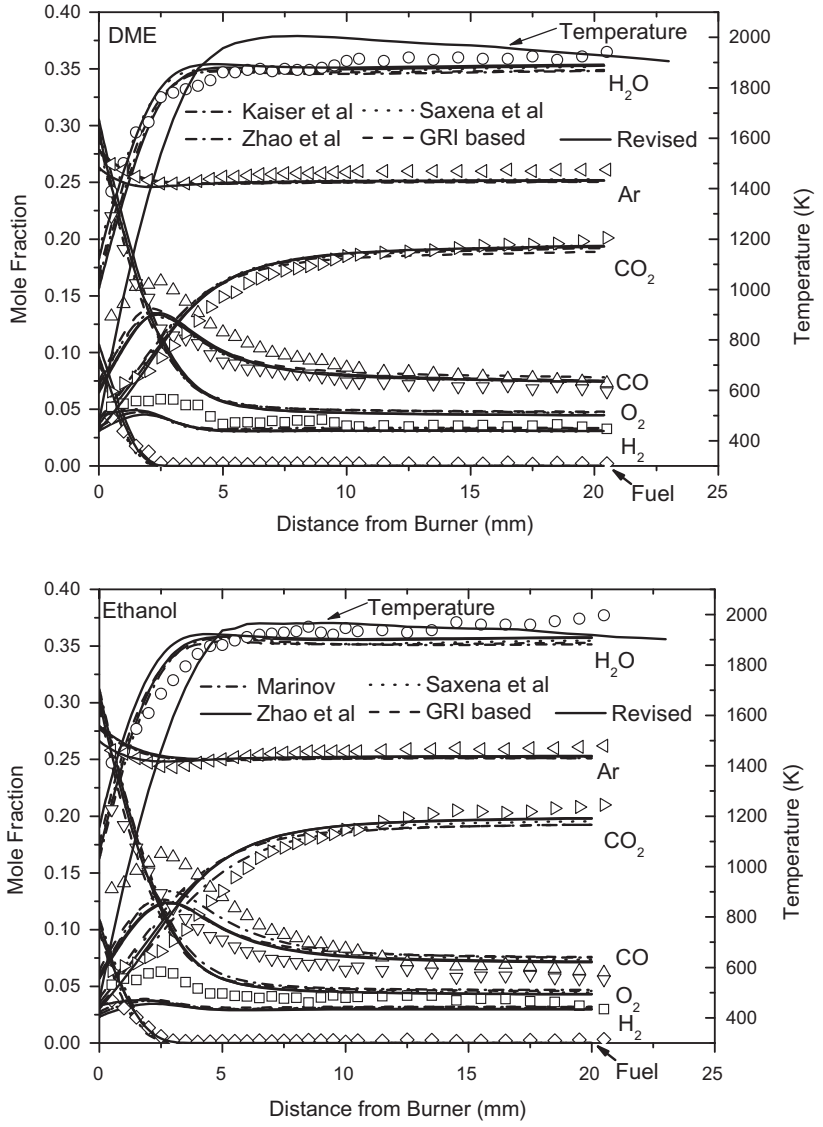

Fig. 2. Temperature and mole fraction of major species profiles in the DME and ethanol flames.

2. Calculate the ion signal of CH_2O at the photoionizaiton energy of 11.8 eV.

$$S(11.8)_{CH_2O}=\frac{X_{CH_2O}S(11.8)_{C_2H_2}\sigma(11.8)_{CH_2O}D_{CH_2O}}{X_{C_2H_2}\sigma(11.8)_{C_2H_2}D_{C_2H_2}}$$

3. Calculate the ion signal of C_2H_6 at the photoionizaiton energy of 11.8 eV.

$$S(11.8)_{C_2H_6}=S(11.8)_{30}-S(11.8)_{CH_2O}$$

Here $S(11.8)_{30}$ is the total measured signal of the species with the molecular weight of 30.

4. Calculate the mole fraction of C_2H_6 at the photoionization energy of 11.8 eV as same as step 1.

Because the ion signal was back calculated at step 3, the uncertainty of the mole fraction of C_2H_6 was then amplified compared with measured ion signal (the uncertainty is about 50%), so this method requires that the species with a higher photoionization threshold must has a relatively high concentration, otherwise it cannot be distinguished or will have a large error. For example, acetaldehyde and propane in the ethanol flame cannot be separated, because the latter whose threshold is high has a very low concentration.

All the C_2 intermediates in the DME flame are less than that in the ethanol flame except ethane, which is the result of methyl combination ($CH_3 + CH_3 \rightarrow C_2H_6$) in both flames, its mole fraction has a well prediction by all mechanisms in the DME flame. In the ethanol flame, however it has a slightly lower prediction, but it is within the error range allowed and is not necessary to revise the mechanism. As for ethylene, the Zhao's mechanism has a major revise. The dehydrogenation reactions in ethane sub-mechanism were replaced by that from the Saxena mechanism, some dehydrogenation reactions of ethane were replaced by from the GRI 3.0 mechanism. The formation reactions of C_2H_4OH in Zhao's mechanism are based on Marinov's mechanism in the revise. Then the modeling mole fraction profiles of ethylene as well as the following acetylene agree with the experiment data better. As for acetaldehyde, Zhao's mechanism has a good prediction in the ethanol flame but a high prediction in the DME flame. The combination of CH_3 and HCO is a major path to produce acetaldehyde in the DME flame. The recent shock tube acetaldehyde pyrolysis

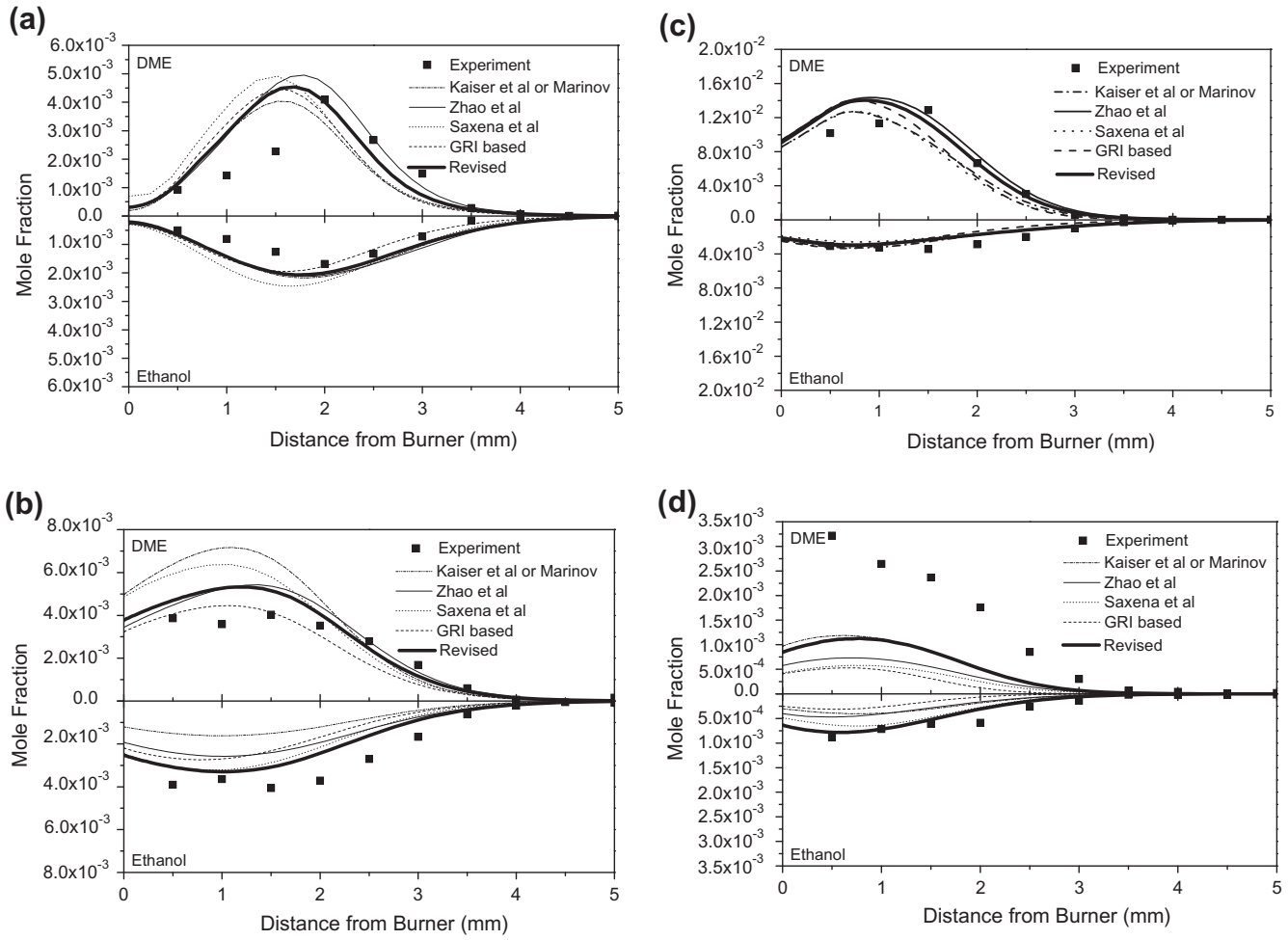

Fig. 3. C_1 intermediates in DME flame (upper) and ethanol flame (lower) mole fraction profiles for (a) methyl radical, (b) methane, (c) formaldehyde and (d) methanol.

study conducted by Yasunaga et al. [42] presents the newest calculated reaction parameters. As Fig. 4d shows it has a well prediction. Ethenol is a species noted by the combustion researchers recently. Current studies show that OH addition to ethylene is the dominant ethenol formation pathway; the unimolecular tautomerization from acetaldehyde to ethenol is not a major pathway [43], and other paths can also be neglected. In this study the ethenol sub-mechanism contains the following five reactions. The rate coefficient of R1 is claimed by Hippler and Viskolcz [44] and Senosiain et al. [45] respectively. The rates of dehydrogenation of ethenol were estimated from that of methanol [11].

$C_2H_4 + OH = C_2H_3OH$	R1 [44,45]
$C_2H_3OH = CH_3HCO$	R2 [46]
$C_2H_3OH + OH = CH_2CHO + H_2O$	R3 [estimated]
$C_2H_3OH + H = CH_2CHO + H_2$	R4 [estimated]
$C_2H_3OH + O = CH_2CHO + OH$	R5 [estimated]

The photoionization cross section of ethenol has been estimated by Cool et al. [12]. The 10.0 eV cross section for ethenol was estimated at 6.4 Mb. From Fig. 4e it can be seen that the modeling results have the right magnitude prediction in both flames, the rate coefficient claimed by Hippler et al. fits the experiment data better, but for the ethanol flame the modeling profile is nearly on the margin of the experimental uncertainty range. Ketene is another common species in most flames [47]. The cross section of this species was estimate based on the cross section for propylene [48]. In the DME flame, it has a well prediction by Zhao's mechanism. In the ethanol flame, the dehydrogenation reaction of CH_2CHO is revised according to the Saxena's mechanism and then has a well prediction.

3.3.3. C_3 intermediates

Although there are several C_3 species can be detected out in both flames, most of them are the by-product and have trace amounts. Some C_3 hydrocarbons such as propane have been included in the mechanism but cannot be separated yet in this study (the reason has been described in the last section). Only ethyl methyl ether (EME) in the DME flame and the species with its molecular weight of 58 in the ethanol flame which have their mole fractions higher than 10^{-4} and can be distinguished are worth to be deliberated, as Fig. 5 shows.

EME was first detected by Cool et al. [8] with its mole fraction of about 8.0×10^{-4} in the $\Phi = 1.2$ DME flame. It is also observed in the stoichiometric ratio DME and ethanol flames in this study. However, it has not been included in current mechanism, the explanation is that there is not reliable EME reaction mechanism available and EME itself is not a major species in the DME oxidation pathway, however the existence of this species might reflect some information of its relative fuel radicals which are difficult to be detected. EME is possibly produced by the CH_3 addition to CH_3OCH_2 in the DME flame and CH_3 addition to C_2H_5O in the ethanol flame on the whole. A shock tube study of EME pyrolysis and oxidation [49] can be referenced to try to describe the EME

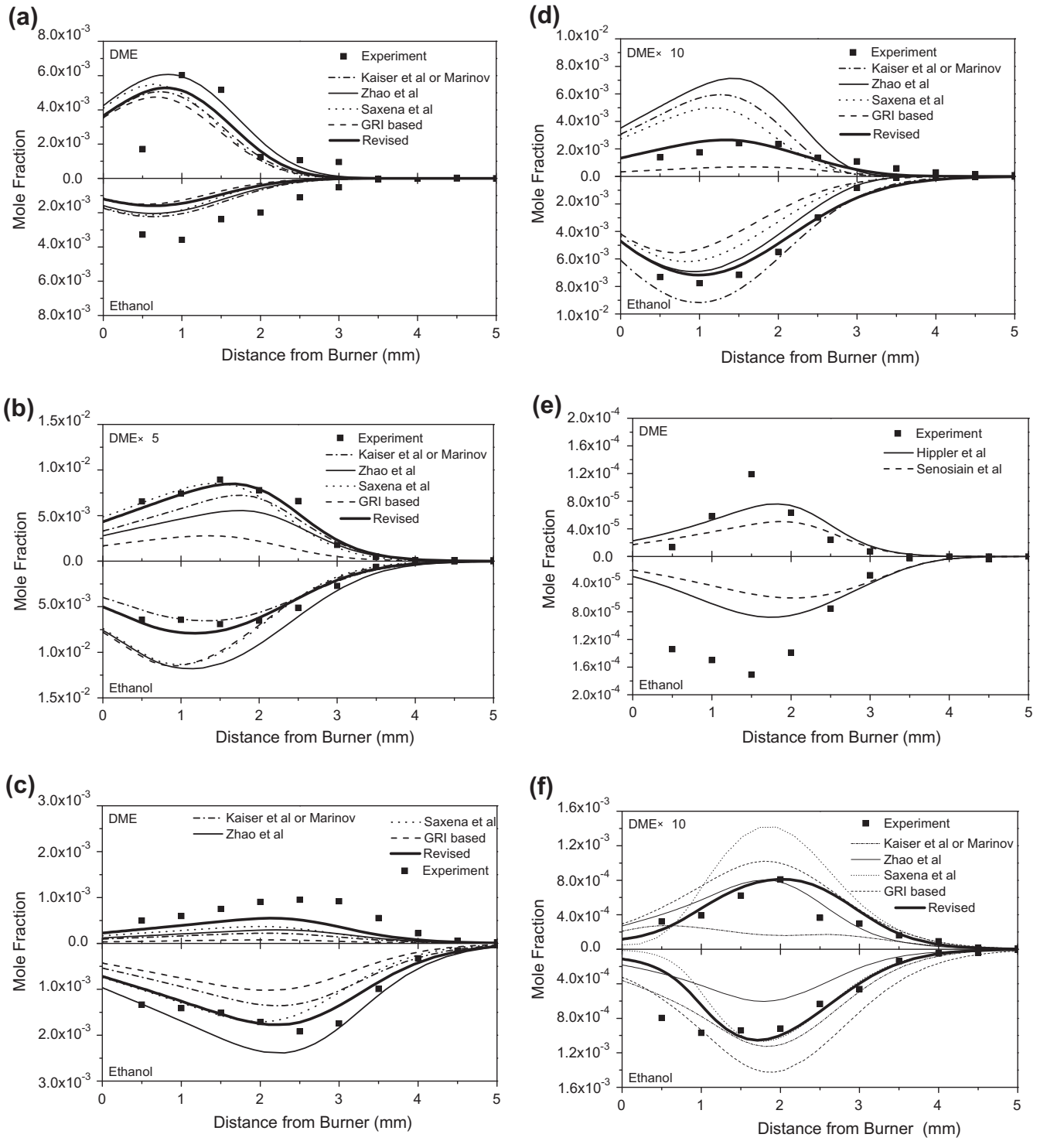

Fig. 4. C_2 intermediates in DME flame (upper) and ethanol flame (lower) mole fraction profiles for (a) ethane, (b) ethylene, (c) acetylene, (d) acetaldehyde, (e) ethenol and (f) ketene.

formation in the DME flame. The photoionization cross section of EME has not been measured, so it is estimate to be 10.0 Mb based on the cross sections for dimethyl ether and diethyl ether [22] at the photoionization energy of 11.0 eV. As Fig. 5a displays, the prediction seems to be reasonable in the ethanol flame but too low in the DME flame. It cannot be declared presently whether the discrepancy is due to mechanism limitation or missing reactions.

The intermediates with $m/z = 58$ and photoionization threshold of 9.70 eV (Fig. 1) can be considered to be acetone and 2-propen-1-ol. As for 2-propen-1-ol, there seems to be no obvious formation pathway, so the photoionizaiton cross section of acetone was used to calculate its mole fraction. The source of acetone is the combination of CH_3 and CH_3CO, the latter is mainly the dehydrogenation product of acetaldehyde. So acetone can be accumulated a sizeable amount in the ethanol flame than in the DME flame. Tow kinds of acetone dissociate reaction rate coefficients provided by Pichon et al. [50] and Saxena et al. [51] respectively were used to describe its formation, and the consumption reactions is provided by Pichon et

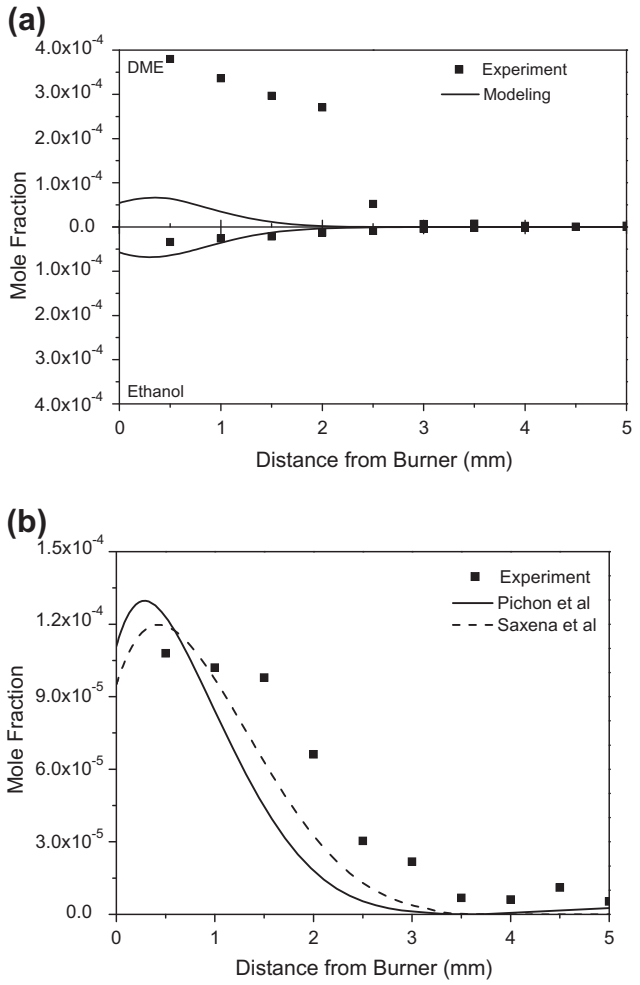

Fig. 5. C_3 intermediates in DME flame (upper) and ethanol flame (lower) mole fraction profiles for (a) EME and (b) acetone (only for ethanol flame).

al. [50]. Since the dehydrogenation ratios by H and OH are 47.9% and 49.5% respectively, other reactions were neglected. As Fig. 5b shows, the prediction by Saxena et al. has a better agreement with the experimental results.

3.4. Reaction path analysis

Figure 6 displays the main reaction pathways of DME and ethanol oxidation and the conversion ratio of each species in the modeling. DME and ethanol are both saturated molecular, so the first step is destroyed by H-abstraction, and direct decompositions are not notable under this low pressure. However, in the following step all dehydrogen products of DME undergo the beta-scission to CH_2O and CH_3, but about half of dehydrogen products of ethanol still lose H-atom and convert to acetaldehyde, so acetaldehyde accumulates to a high concentration in the ethanol flame while formaldehyde has a high concentration in the DME flame. The following reactions are more complex in the ethanol flame than in the DME flame, but finally all species in the both flames end in CH_2O. Overall the minor revisions just to aim at the branch path, so the main paths of the carbon flux in both flames are not interfered. The only difference exists in the decomposition of ethanol, by including the low pressure sub-mechanism of Saxnea et al., this path trend to be narrow. The flux of C2 hydrocarbon has some appreciable changes, more carbon toward to dehydrogenation rather than decomposition to methyl; the dehydrogen product of acetaldehyde also tend to further dehydrogenation to produce ketene rather than decomposition; besides, the formation of acetaldehyde in the DME flame which is not shown in the figure has a low tendency and the formation of methanol in both flames has a high tendency compared with the previous prediction. It can be seen all of these changes are concerned with the pressure dependent unimolecular fall-off reactions (e.g. $C_2H_5OH=C_2H_4+OH$) or chemically activated bimolecular reactions (e.g. $C_2H_5+O=CH_3+CH_2O$). So perhaps the revises are actually for pressure specially.

4. Other validations

In order to validate the revised mechanism comprehensively, sever validation experiments conducted by others were adopted in test also. For DME flame, two DME/O_2/Ar flames with the equivalence ratio of 1.2 and 1.68 in Cool's study and selected other two DME/O_2/Ar flames with the equivalence ratio of 0.93 and 1.4 in Wang's study were chosen for validation. However surprisingly, there are only few data available on ethanol flame structures. In addition the measurement techniques are seem to be not as accurate and advanced as the DME flames. Here only a stoichiometric ratio ethanol/O_2/Ar flame in Kasper's study was chosen. The results of modeling by using revised mechanism and Zhao's mechanism are shown in Supplementary material 2.

For methyl and methane, the validations experiments of others show that the revise indeed decreases the difference between the experiment and modeling in either DME flames or ethanol flame, especially for methane (as Fig. S2-1 shown). For methyl radical, the modeling result still has large inconformity by contrast with Wang's study and Ksaper's study, but the prediction is basically correct for Cool's study. However, for both species the gap increases with the increase of equivalence ratio. No revises was made for formaldehyde as the original mechanism has made the acceptable predictions for all flames. The study of methanol still need to be proceeded since the variation tendency between the experiment and modeling with the change of equivalence ratio is opposite, although the prediction is improved for some flames (Fig. S2-2).

Ethane in this study and Cool's flames has well predications, however in Wang's flame, it is over predicted by twice than that from experiment result, therefore, no obvious revision can be made. In this study ethylene is underestimated in the DME flame but overestimated in the ethanol flame, so the corresponding revise has been made. From Fig. S2-2 it can be seen the prediction was improved in all flames, and in the ethanol flame, although the prediction is decreased greatly, large difference between experiment and modeling still exists. While the value of the experiment result seems to be too low to be accepted, since ethylene is a major species in one of the three carbon fluxes which shares about a quarter of carbon in the ethanol flame as Fig. 6b shown. The following dehydrogen product of acetylene is also thought to be too low, nevertheless the revise has the fairly accurate predictions in the DME flames. Acetaldehyde (Fig. S2-3) in the DME flames is all overestimated by previous mechanisms, the revised mechanism decrease this over prediction and has an excellence agreement with experiment for either DME flames or ethanol flame. The last one ketene has minimum amounts in the DME flames, in Wang's flames it is all overestimated, but has well prediction in this study and Cool's flames.

5. Summary and conclusions

Using a molecular-beam flame-sampling photoionization mass spectrometry combining with the synchrotron radiation and the simulation code PREMIX, the comparisons of high temperature

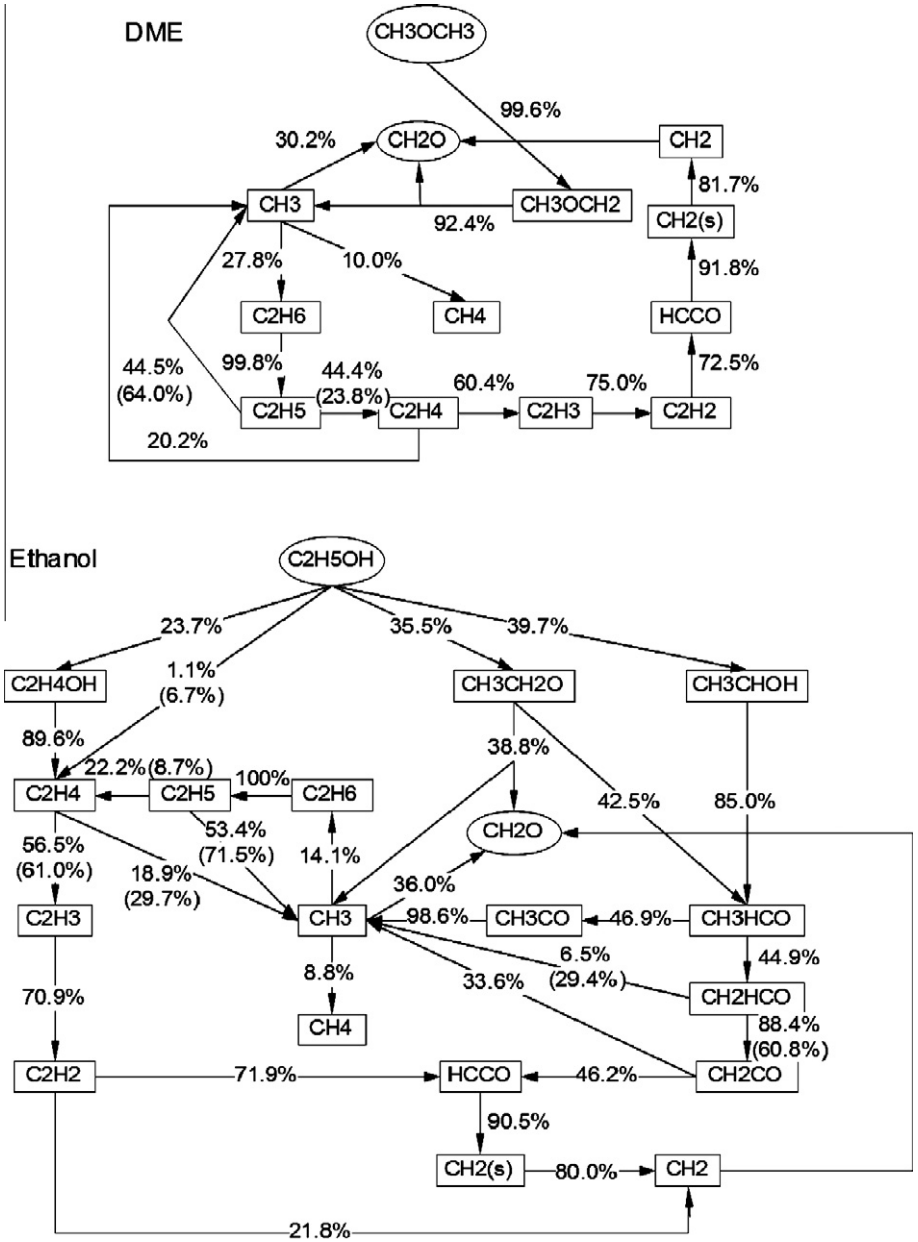

Fig. 6. Main consumption pathways and species conversion ratio of species in the DME and ethanol flames modeling by using the revised mechanism. The percentages in the bracket are the calculation results by using Zhao's mechanism. All of these values shown have differences large than 5% compared with the revised results.

oxidation in the new low pressure stoichiometric ratio laminar premixed DME/O_2/Ar and ethanol/O_2/Ar flames were conducted. The temperature profiles and mole fraction profiles of major species as well as some other species with their mole fractions higher than 10^{-4} were compared and analyzed. Five mechanisms were introduced in the modeling study for validation. Based on the mechanism developed by Zhao et al., by a slight revision the modeling accuracy was increased and the modeling results well agree with the experiment result. The mole fraction profiles of some species including ethenol, acetone and ethyl methyl ether (EME) which have not been included in current mechanism has also been simulated. Methanol and EME were underestimated obviously by current model in the DME flame, probably due to the lack of reactions or mechanism problem, their reaction paths should be studied for further investigation. The reaction path and species conversion ratio analysis show that the revised mechanism mainly aims at the pressure dependent reactions. Meanwhile, the revised mechanism was also validated by several low pressure flames in others' study, including four DME/O_2/Ar flames and one ethanol/O_2/Ar flame. The improvements can be clear seen in all flames by using the revised mechanism.

Acknowledgments

The authors acknowledge the financial support by the Natural Science Foundation of China (No. 50876075) and the Foundation of the Ministry of Education of China (No. 200800560040). We'd also like to thank Prof. Fei Qi and his assistants at the combustion and flame endstation of National Synchrotron Radiation Laboratory, University of Science and Technology of China in the experiment.

Appendix A. Supplementary material

Supplementary data associated with this article can be found, in the online version, at doi:10.1016/j.combustflame.2011.01.004.

References

[1] C. Beatrice, C. Bertoli, N.D. Giacomo, Combust. Sci. Technol. 137 (1998) 31–50.
[2] K.H. Song, P. Nag, T.A. Litzinger, D.C. Haworth, Combust. Flame 135 (2003) 341–349.
[3] C. Esarte, Á. Millera, R. Bilbao, M.U. Alzueta, Ind. Eng. Chem. Res. 49 (2010) 6772–6779.
[4] D.M. Jiang, Z.H. Huang, Alternative Fuel Combustion for Internal Combustion Engine, Xi'an Jiaotong University Press, Xi'an, 2007.
[5] A. McIlroy, T.D. Hain, H.A. Michelsen, T.A. Cool, Proc. Combust. Inst. 28 (2000) 1647–1653.
[6] N. Leplat, A. Seydi, J. Vandooren, Combust. Sci. Technol. 180 (2008) 519–532.
[7] T.S. Kasper, P. Oßwald, M. Kamphus, K. Kohse-Höinghaus, Combust. Flame 150 (2007) 220–231.
[8] T.A. Cool, J. Wang, N. Hansen, P.R. Westmoreland, F.L. Dryer, Z.W. Zhao, A. Kazakov, T. Kasper, K. Kohse-Höinghaus, Proc. Combust. Inst. 31 (2007) 285–293.
[9] J. Wang, M. Chaos, B. Yang, T.A. Cool, F.L. Dryer, T. Kasper, N. Hansen, P. Oßwald, K. Kohse-Höinghaus, Phys. Chem. Chem. Phys. 11 (2009) 1328–1339.
[10] J. Wang, U. Struckmeier, B. Yang, T.A. Cool, P. Oßwald, K. Kohse-Höinghaus, T. Kasper, N. Hansen, P.R. Westmoreland, J. Phys. Chem. A 112 (2008) 9255–9265.
[11] Z.W. Zhao, M. Chaos, A. Kazakov, F.L. Dryer, Int. J. Chem. Kinet. 40 (2008) 1–18.
[12] T.A. Cool, K. Nakajima, T.A. Mostefaoui, F. Qi, A. McIlroy, P.R. Westmoreland, M.E. Law, L. Poisson, D.S. Peterka, M. Ahmed, J. Chem. Phys. 119 (2003) 8356–8365.
[13] T.A. Cool, A. McIlroy, F. Qi, P.R. Westmoreland, L. Poisson, D.S. Peterka, M. Ahmed, Rev. Sci. Instrum. 76 (2005) 094102.
[14] N. Hansen, T.A. Cool, P.R. Westmoreland, K. Kohse-Höinghaus, Prog. Energy Combust. Sci. 35 (2009) 168–191.
[15] F. Qi, R. Yang, B. Yang, C.Q. Huang, L.X. Wei, J. Wang, L.S. Sheng, Y.W. Zhang, Rev. Sci. Instrum. 77 (2006) 084101.
[16] B. Yang, Y.Y. Li, L.X. Wei, C.Q. Huang, J. Wang, Z.Y. Tian, R. Yang, L.S. Sheng, Y.W. Zhang, F. Qi, Proc. Combust. Inst. 31 (2007) 555–563.
[17] B. Yang, P. Owald, Y.Y. Li, J. Wang, L.X. Wei, Z.Y. Tian, F. Qi, Combust. Flame 148 (2007) 198–209.
[18] C.D. Yao, J. Li, Q. Li, C.Q. Huang, L.X. Wei, J. Wang, Z.Y. Tian, Y.Y. Li, F. Qi, Chemosphere 67 (2007) 2065–2071.
[19] T.A. Cool, K. Nakajima, C.A. Taatjes, Proc. Combust. Inst. 30 (2005) 1681–1688.
[20] C.A. Taatjes, D.L. Osborn, T.M. Selby, G. Meloni, H.Y. Fan, S.T. Pratt, J. Phys. Chem. A 112 (2008) 9336–9343.
[21] J. Wang, B. Yang, T.A. Cool, N. Hansen, T. Kasper, Int. J. Mass Spectrom. 269 (2008) 210–220.
[22] T.A. Cool, J. Wang, K. Nakajima, C.A. Taatjes, A. McIlroy, Int. J. Mass Spectrom. 247 (2005) 18–27.
[23] G. Cooper, J.E. Anderson, C.E. Brion, Chem. Phys. 209 (1996) 61–77.
[24] J.H. Kent, Combust. Flame 14 (1970) 279–281.
[25] R.A. Shandross, J.P. Longwell, J.B. Howard, Combust. Flame 85 (1991) 282–284.
[26] M. Fristrom, Flame Structure and Processes, Oxford, New York, 1995.
[27] A.T. Hartlieb, B. Atakan, K. Kohse-Höinghaus, Combust. Flame 121 (2000) 610–624.
[28] J.C. Biordi, C.P. Lazzara, J.F. Papp, Combust. Flame 23 (1974) 73–82.
[29] R.J. Cattolica, S. Yoon, E.L. Knuth, Combust. Sci. Technol. 28 (1982) 225–239.
[30] U. Struckmeier, P. Oßwald, T. Kasper, L. Böhling, M. Heusing, M. Köhler, A. Brockhinke, K. Kohse-Höinghaus, Z. Phys. Chem. 223 (2009) 503–537.
[31] R.J. Kee, J.F. Grcar, M.D. Smooke, J.A. Miller, Report No. SAND85-8240, Sandia National Laboratories, 1985.
[32] E.W. Kaiser, T.J. Wallington, M.D. Hurley, J. Platz, H.J. Curran, W.J. Pitz, C.K. Westbrook, J. Phys. Chem. 104 (2000) 8194–8206.
[33] N.M. Marinov, Int. J. Chem. Kinet. 31 (1999) 183–220.
[34] J. Li, Experimental and Numerical Studies of Ethanol Chemical Kinetics, PhD thesis, Princeton University, 2004.
[35] P. Saxena, F.A. Williams, Proc. Combust. Inst. 31 (2007) 1149–1156.
[36] G.P. Smith, D.M. Golden, M. Frenklach, N.W. Moriarty, B. Eiteneer, M. Goldenberg, C.T. Bowman, R.K. Hanson, S. Song, W.C. Gardiner, Jr., V.V. Lissianski, Z. Qin. <http://www.me.berkeley.edu/gri_mech/>.
[37] C.A. Taatjes, N. Hansen, A. McIlroy, J.A. Miller, J.P. Senosiain, S.J. Klippenstein, F. Qi, L.S. Sheng, Y.W. Zhang, T.A. Cool, J. Wang, P.R. Westmoreland, M.E. Law, T. Kasper, K. Kohse-Höinghaus, Science 308 (2005) 1887–1889.
[38] <http://webbook.nist.gov/chemistry/>.
[39] S.S. Yoon, D.H. Anh, S.H. Chung, Combust. Flame 154 (2008) 368–377.
[40] C.S. McEnally, L.D. Pfefferle, Proc. Combust. Inst. 31 (2007) 603–610.
[41] J. Li, A. Kazakov, M. Chaos, F.L. Dryer, Chemical Kinetics of Ethanol Oxidation, 5th US Combustion Meeting, Western States Section of the Combustion Institute, San Diego, 2007.
[42] K. Yasunaga, S. Kubo, H. Hoshikawa, T. Kamesawa, Y. Hidaka, Int. J. Chem. Kinet. 40 (2008) 73–102.
[43] L.K. Huynh, H.R. Zhang, S.W. Zhang, E. Eddings, A. Sarofim, M.E. Law, P.R. Westmoreland, T.N. Truong, J. Phys. Chem. A 113 (2009) 3177–3185.
[44] H. Hippler, B. Viskolcz, Phys. Chem. Chem. Phys. 2 (2000) 3591–3596.
[45] J.P. Senosiain, S.J. Klippenstein, J.A. Miller, J. Phys. Chem. A 110 (2006) 6960–6970.
[46] G. Silva, C. Kim, J.W. Bozzelli, J. Phys. Chem. A 110 (2006) 7925–7934.
[47] C.S. Mcenally, Proc. Combust. Inst. 28 (2000) 2063–2070.
[48] J.C. Person, P.P. Nicole, J. Chem. Phys. 53 (1968) 1767–1970.
[49] K. Yasunaga, T. Koike, H. Hoshikawa, Y. Hidaka, Proc. Combust. Inst. 31 (2007) 313–320.
[50] S. Pichon, G. Black, N. Chaumeix, M. Yahyaoui, J.M. Simmie, H.J. Curran, R. Donohue, Combust. Flame 156 (2009) 494–504.
[51] S. Saxena, J.H. Kiefer, S.J. Klippenstein, Proc. Combust. Inst. 32 (2009) 123–130.